Raman and two-plasmon decay instabilities in a magnetized plasma

H. C. Barr, T. J. M. Boyd, L. R. T. Gardner, and R. Rankin
University of Wales, UCNW, Bangor, Wales

(Received 21 September 1981; accepted 15 March 1984)

The effects of a magnetic field on the Raman and two-plasmon decay instabilities are studied in the region of the quarter-critical density of laser produced plasmas where both are coincident. Two-plasmon decay of the incident extraordinary wave into two upper-hybrid waves may now occur in the direction of propagation of the incident radiation driven by the electrostatic component of the extraordinary mode. Maximum growth rates of both the Raman and two-plasmon decay instabilities are increased by the magnetic field. For the two-plasmon decay, the frequency shift from $\omega_0/2$, where ω_0 is the frequency of the incident radiation, is increased by the magnetic field by amounts which can exceed the thermal shift. This magnetic shift derives from the electromagnetic correction to the dispersion relation of upper-hybrid waves and, consequently, is not found in an electrostatic approximation. For the Raman instability at the reflection point of the scattered extraordinary wave, the red shift of the back-scattered radiation due to the plasma temperature is reduced by any magnetic field present and can be changed to a blue shift if the field is large enough.

I. INTRODUCTION

In studies of laser-plasma interactions, considerable attention has been paid to the underdense coronal region in view of its importance in scattering the incident light or, through processes such as filamentation, in corrupting the uniformity of the target irradiation. Within the underdense plasma one region of special significance is that surrounding the quarter-critical density since it is here that stimulated Raman scattering, the decay of the incident radiation into a longitudinal plasma wave and a scattered electromagnetic wave, and two-plasmon decay, in which the products are both longitudinal waves, occur. Although both processes have already been widely studied there is nevertheless continued interest in each of them, and in stimulated Brillouin scattering and filamentation too, in view of the extensive underdense regions characteristic of the ablative compression of targets.

Stimulated Raman scattering has been considered theoretically and in computer experiments by a number of authors.[1–5] The frequency matching condition demands that the frequency of the scattered radiation $\omega_2 \simeq \omega_0 - \omega_1$, where ω_0 is the frequency of the incident radiation and ω_1 is that of the electron plasma wave. In a cold plasma the scattered radiation frequency $\omega_2 \geqslant \omega_0/2$. Recent computer experiments by Kruer *et al.*[5] have shown that in a hot plasma the high temperature can produce a frequency shift in the spectrum of scattered radiation to frequencies below $\omega_0/2$. The shifts predicted are high enough to be easily detected and, if measured, could provide an indication of the plasma temperature in the quarter-critical density zone.

Two-plasmon decay was first examined for homogeneous plasmas[6,7] and in the context of laser plasma interaction studies was extended to inhomogeneous plasmas by Rosenbluth,[8] Lee and Kaw,[9] Liu and Rosenbluth,[10] and Schuss.[11] The instability threshold in inhomogeneous plasmas is lower than that for stimulated Raman scattering. The saturation of the two-plasmon instability has been examined by Langdon *et al.*[12] in computer experiments.

Phenomena at the quarter-critical density are manifest in radiation emitted from that region at half-integral harmonics of the laser frequency, although there is also some limited direct evidence of the occurrence of large amplitude electron plasma waves near quarter critical and of modifications to the electron density profile in experiments by Baldis *et al.*[13] There is now widespread evidence of the presence of plasma waves in this region from observations of emission at $3\omega_0/2$ in the backscattered light.[14–18] Typically, $3\omega_0/2$ spectra obtained by Carter *et al.*[18] consisted of a broad feature with a red and a blue wing. The separation between these two peaks tended to decrease with time and eventually to coalesce. In experiments with a larger prepulse (and consequently, a less steep density gradient during the main pulse) the spectral separation first increased before decreasing. The red and blue wings were approximately equally sited with respect to the line center.

Avrov *et al.*[19] considered two-plasmon decay as a source for the emission at $3\omega_0/2$, either through interaction with an incident photon or by three-plasmon recombination. This process has been reconsidered by Barr[18] who obtained an expression for the spectral width of the doublet which differs in detail from the result of Avrov *et al.* Both theories relate the separation to the electron temperature, but to obtain agreement with the widths measured by Carter *et al.* the model developed by Avrov *et al.* requires an unrealistically high value to be taken for the electron temperature, whereas in Barr's result this requirement is relaxed by a factor of about three.

So far, we have only considered unmagnetized plasma. However, recent experiments[20–25] have established the presence of very large, if highly localized, magnetic fields in plasmas created by the irradiation of solid targets by high intensity lasers. Among the most extensive studies undertaken so far are those of Raven *et al.*[24] who have examined the effect of target size and composition on the generation of thermoelectrically driven magnetic fields, using a single beam of the neodymium glass laser at the Rutherford and Appleton Lab-

 0031-9171/84/112730-08$01.90

oratories. A range of target plasmas was observed with Faraday rotation measurements using a fourth harmonic probe beam, allowing magnetic fields to be measured at densities up to critical.

Strong magnetic fields in the megagauss range were seen from large plane targets. The experimental results show that the thermo-electrically generated field at the edge of the focal spot rises from zero at the refractive cutoff to about 600 kG at the critical density and increases steadily to just over 3 MG at $0.2\,N_c$ before dropping steeply to zero around $0.1N_c$. The main conclusion from this work is that the strongest fields are to be found in the low-density coronal plasma.

The existence of fields of this magnitude in the neighborhood of the quarter-critical density suggests that there may be observable effects because of their presence in laser–plasma interactions in that region. Parametric processes in laser-produced plasmas in which strong magnetic fields are present have not been widely studied. There are, of course, many papers on three wave interactions in magnetized plasmas viewed in a wider context.[26–29] Kaw[30] has considered the decay of a left circularly polarized electromagnetic pump propagating along a constant uniform magnetic field into a scattered electromagnetic wave and an ion-acoustic wave. However, that polarization is not particularly relevant to laser-produced plasmas in which a self-generated field is present. Since these fields are generated in the main by the so-called $\nabla N \times \nabla T$ source, and the principal density gradient is aligned along the laser direction, one should properly consider the geometry in which the incident radiation propagates across the magnetic field.

In two recent papers, Grebogi and Liu[31,32] have considered stimulated Raman scattering and the parametric decay of an extraordinary electromagnetic wave into two upper-hybrid plasmons. However, neither is adequate to deal with the effects of a self-generated magnetic field in a laser-produced plasma. In the work on stimulated Raman scattering, for example, it is assumed that the frequency of the upper-hybrid wave is much less than that of the pump or the scattered extraordinary mode. This has the consequence that their treatment is valid in the underdense plasma away from the quarter-critical density. The upper-hybrid wave is treated electrostatically, i.e., the phase velocity is much less than the velocity of light.

In this paper we shall examine the effect of a magnetic field on the decay of an extraordinary pump wave into an upper-hybrid wave and either a scattered extraordinary wave (stimulated Raman scattering) or another upper-hybrid mode (two-plasmon decay). A general fully electromagnetic dispersion relation is derived, valid for any plasma density and temperature, pump power, and magnetic field $\mathbf{B}_c$. (Although self-generated fields have a complicated morphology,[24,33] we shall assume in this work that $\mathbf{B}_c$ is both constant and uniform.) However, we are interested first and foremost in the region near quarter critical where stimulated Raman scattering and two-plasmon decay are coincident and where a purely electrostatic treatment of upper-hybrid waves is inadequate. This is a complex region, rich in physical effects, the details of which are only represented accurately by the electromagnetic dispersion relation. This adds considerably to the algebraic complexity, and we have had to treat the full dispersion relation numerically.

The coupled mode equations are derived in Sec. II together with a brief discussion of the numerical analysis of the dispersion relation. The results of the analysis are presented and discussed in Sec. III and the principal conclusions together with some limitations of the present work reviewed in Sec. IV.

II. THE COUPLED MODE EQUATIONS

We wish to solve the coupled mode equations describing the decay of an extraordinary wave into an upper-hybrid wave and either a scattered extraordinary wave or a second upper-hybrid wave, using the fluid equations

$$\frac{\partial n}{\partial t} + \nabla \cdot (n\mathbf{v}) = 0, \tag{1}$$

$$\frac{\partial \mathbf{v}}{\partial t} = -\frac{e}{m}\mathbf{E} + \mathbf{v}\times\left(\nabla\times\mathbf{v} - \frac{e}{mc}\mathbf{B}\right) - \nabla\left(\frac{v^2}{2}\right) - 3V_e^2\frac{\nabla n}{n}, \tag{2}$$

together with Maxwell's equations. The ions are assumed to be immobile and the unperturbed plasma homogeneous. Here $\mathbf{E}$ and $\mathbf{B}$ are the electric and magnetic fields, respectively, $\mathbf{v}$ is the fluid velocity, n is the number density and e, m are the electron charge and mass. The electron thermal velocity $V_e = (T_e/m)^{1/2}$, where T_e is the electron temperature and c is the velocity of light.

Rather than merely quote the familiar expression for extraordinary waves, we shall derive a dispersion relation which also describes upper-hybrid waves including electromagnetic corrections to the usual electrostatic dispersion relation

$$\omega^2 = \omega_p^2 + \Omega_c^2 + 3k^2V_e^2, \tag{3}$$

in which $\Omega_c = eB_c/mc$. In what follows we shall see that this correction can give rise to observable frequency shifts.

Let $n = N_0 + n_0$, where N_0 is the number density of the unperturbed electrons while n_0 is the oscillating density resulting from the electric field in the direction of propagation. For an extraordinary wave this field arises from the Lorentz force ($n_0 = 0$ when $\mathbf{B}_c = 0$). The extraordinary and upper-hybrid waves are described in the fluid approximation by the set of equations:

$$\frac{\partial n_0}{\partial t} + N_0\nabla\cdot\mathbf{v}_0 = 0, \tag{4}$$

$$\frac{\partial \mathbf{v}_0}{\partial t} = -\frac{e}{m}\mathbf{E}_0 - \mathbf{v}_0\times\boldsymbol{\Omega}_c - 3V_e^2\frac{\nabla n_0}{N_0}, \tag{5}$$

$$\frac{\partial \mathbf{B}_0}{\partial t} = -c\nabla\times\mathbf{E}_0, \tag{6}$$

$$\frac{\partial \mathbf{E}_0}{\partial t} = c\nabla\times\mathbf{B}_0 + 4\pi eN_0\mathbf{v}_0, \tag{7}$$

in which harmonic terms have been neglected. Assuming propagation in the x direction, we see at once for extraordinary and upper-hybrid waves (i.e., E_0, v_0 perpendicular to B_c and B_0 parallel to B_c, respectively) that $\{E_{0y}, B_0, v_{0x}, n_0\}$ are $\pi/2$ out-of-phase with $\{E_{0x}, v_{0y}\}$. Consequently, we may set $\{E_{0y}, B_0, v_{0x}, n_0\} = \{E_{0y}, B_0, v_{0x}, n_0\}\cos(k_0x - \omega_0t)$,

$\{E_{0x}, v_{0y}\} = \{E_{0x}, v_{0y}\} \sin(k_0 x - \omega_0 t)$. Then, (4)–(6) give $B_0 = ck_0 E_{0y}/\omega_0$; $n_0 = -k_0 E_{0x}/4\pi e$,

$$v_{0x} = \frac{-e/m}{\omega_0^2 - \Omega_c^2}\left[\omega_0 E_{0x}\left(1 + \frac{3k_0^2 V_e^2}{\omega_p^2}\right) + \Omega_c E_{0y}\right], \tag{8}$$

$$v_{0y} = \frac{e/m}{\omega_0^2 - \Omega_c^2}\left[\omega_0 E_{0y} + \Omega_c\left(1 + \frac{3k_0^2 V_e^2}{\omega_p^2}\right)E_{0x}\right], \tag{9}$$

where $\omega_p^2 = 4\pi N_0 e^2/m$. Finally, (7) yields

$$E_{0x} = \frac{\Omega_c \omega_p^2/\omega_0}{\omega_0^2 - \omega_p^2 - \Omega_c^2 - 3k_0^2 V_e^2} E_{0y}, \tag{10}$$

and the dispersion relation

$$(\omega_0^2 - \omega_p^2 - \Omega_c^2 - 3k_0^2 V_e^2)(\omega_0^2 - \omega_p^2 - k_0^2 c^2) - \Omega_c^2 \omega_p^2 = 0. \tag{11}$$

The high-frequency branch in (11) represents the extraordinary wave; the lower branch corresponds to the upper-hybrid mode.

Note that by neglecting the $\Omega_c^2 \omega_p^2$ term we retrieve the electrostatic upper-hybrid dispersion relation (3), although the dispersion relation for the extraordinary wave is not given correctly by this approximation.

Next consider the first-order equations, assuming that the pump is an extraordinary wave satisfying (11), and

$$\mathbf{E}_0 = E_{0x}\hat{\mathbf{x}} \sin(k_0 x - \omega_0 t) + E_{0y}\hat{\mathbf{y}} \cos(k_0 x - \omega_0 t). \tag{12}$$

Let

$$n = N_0 + n_1, \quad \mathbf{v} = \mathbf{v}_0 + \mathbf{v}_1,$$
$$\mathbf{E} = \mathbf{E}_0 + \mathbf{E}_1, \quad \mathbf{B} = \mathbf{B}_c + \mathbf{B}_0 + \mathbf{B}_1. \tag{13}$$

The first-order equations are

$$\frac{\partial \mathbf{v}_1}{\partial t} + \mathbf{v}_1 \times \boldsymbol{\Omega}_c + \frac{e}{m}\mathbf{E}_1 + 3V_e^2 \frac{\nabla n_1}{N_0}$$
$$= -\nabla(\mathbf{v}_0 \cdot \mathbf{v}_1) + \mathbf{v}_0 \times [\nabla \times \mathbf{v}_1 - (e/mc)\mathbf{B}_1]$$
$$+ \mathbf{v}_1 \times [\nabla \times \mathbf{v}_0 - (e/mc)\mathbf{B}_0], \tag{14}$$

$$\frac{\partial \mathbf{B}_1}{\partial t} + c\nabla \times \mathbf{E}_1 = 0, \tag{15}$$

$$\frac{\partial \mathbf{E}_1}{\partial t} - c\nabla \times \mathbf{B}_1 - 4\pi e N_0 \mathbf{v}_1 = 4\pi e(n_0 \mathbf{v}_1 + n_1 \mathbf{v}_0), \tag{16}$$

$$\nabla \cdot \mathbf{E} = -4\pi e n_1. \tag{17}$$

Fourier analyzing Eqs. (14)–(17) and dropping the subscripts on the first-order Fourier analyzed quantities, we find, using

$$\mathbf{B} = c\mathbf{k} \times \mathbf{E}/\omega; \quad i\mathbf{k} \cdot \mathbf{E} = -4\pi e n,$$

that (16) gives

$$c^2 \mathbf{k}(\mathbf{k} \cdot \mathbf{E}) - (k^2 c^2 - \omega^2)\mathbf{E} - 4\pi e i\omega N_0 \mathbf{v}$$
$$= 4\pi e i\omega \mathcal{F}(n_0 \mathbf{v}_1 + n_1 \mathbf{v}_0), \tag{18}$$

while (14) becomes

$$-i\omega \mathbf{v} + \mathbf{v} \times \boldsymbol{\Omega}_c + (e/m)\mathbf{E} + 3iV_e^2 \mathbf{k}(n/N_0)$$
$$= -i\mathbf{k}\mathcal{F}(\mathbf{v}_0 \cdot \mathbf{v}_1) + \mathcal{F}\{\mathbf{v}_0 \times [\nabla \times \mathbf{v}_1 - (e/mc)\mathbf{B}_1]$$
$$+ \mathbf{v}_1 \times [\nabla \times \mathbf{v}_0 - (e/mc)\mathbf{B}_0]\}, \tag{19}$$

where $\mathcal{F}(\cdot) = \int d\mathbf{r}\, dt \exp[i(\omega t - k \cdot r)](\cdot)$. The coupling terms become, on setting $\mathbf{k}_\pm = \mathbf{k} \pm \mathbf{k}_0$, $\omega_\pm = \omega \pm \omega_0$, and $f(\mathbf{k}_\pm, \omega_\pm) = f_\pm$ for any first-order quantity f,

$$\mathcal{F}(n_0 \mathbf{v}_1 + n_1 \mathbf{v}_0) = \tfrac{1}{2} n_0(\mathbf{v}_- + \mathbf{v}_+) + \tfrac{1}{2}(\mathbf{V}_0 n_- + \mathbf{V}_0^* n_+), \tag{20}$$

$$\mathcal{F}(\mathbf{v}_0 \cdot \mathbf{v}_1) = \tfrac{1}{2}(\mathbf{V}_0 \cdot \mathbf{v}_- + \mathbf{V}_0^* \cdot \mathbf{v}_+), \tag{21}$$

$$\mathcal{F}\{\mathbf{v}_0 \times [\nabla \times \mathbf{v}_1 - (e/mc)\mathbf{B}_1]\}$$
$$= \tfrac{1}{2}\{\mathbf{V}_0 \times [\mathbf{k}_- \times \mathbf{v}_- + (ie/mc)\mathbf{B}_-]$$
$$+ \mathbf{V}_0^* \times [k_+ \times \mathbf{v}_+ - (ie/mc)\mathbf{B}_+]\}, \tag{22}$$

$$\mathcal{F}\{\mathbf{v}_1 \times [\nabla \times \mathbf{v}_0 - (e/mc)\mathbf{B}_0]\}$$
$$= \tfrac{1}{2}(\mathbf{v}_- + \mathbf{v}_+) \times [\mathbf{k}_0 \times \mathbf{v}_0 - (e/mc)\mathbf{B}_0], \tag{23}$$

where $\mathbf{V}_0 = v_{0x}\hat{\mathbf{x}} - iv_{0y}\hat{\mathbf{y}}$. To simplify the notation, we normalize all lengths to ω_0/c, times to $1/\omega_0$, velocities to c, i.e., let

$$c\mathbf{k}/\omega_0 \to \mathbf{k}, \quad \omega/\omega_0 \to \omega, \quad \mathbf{v}/c \to \mathbf{v}, \quad \omega_p/\omega_0 \to \omega_p,$$
$$n/N_0 \to n, \quad e\mathbf{E}/m\omega_0 c \to \mathbf{E}, \quad e\mathbf{B}/m\omega_0 c \to \mathbf{B}.$$

Henceforth, we presuppose this normalization for all quantities.

Further, assuming that $(\omega_+, \mathbf{k}_+)$ is nonresonant and that the pump wave $(1, \mathbf{k}_0)$ decays into waves $(\omega, \mathbf{k})$ and $(\omega_-, \mathbf{k}_-)$, we obtain the coupled mode equations in the form required for our analysis, i.e.,

$$(k^2 - \omega^2)\mathbf{E} - \mathbf{k}(\mathbf{k} \cdot \mathbf{E}) + i\omega\omega_p^2 \mathbf{v} = -(i/2)\omega\omega_p^2(n_0 \mathbf{v}_- + \mathbf{V}_0 n_-), \tag{24}$$

$$-i\omega \mathbf{v} + \mathbf{v} \times \boldsymbol{\Omega}_c + \mathbf{E} + 3iV_e^2 \mathbf{k} n$$
$$= -(i/2)\mathbf{k}\mathbf{V}_0 \cdot \mathbf{v}_- + (i/2)\mathbf{V}_0 \times (\mathbf{k}_- \times \mathbf{v}_- + i\mathbf{B}_-)$$
$$+ \tfrac{1}{2}\mathbf{v}_- \times (\mathbf{k}_0 \times \mathbf{v}_0 - \mathbf{B}_0), \tag{25}$$

$$(k_-^2 - \omega_-^2)\mathbf{E}_- - \mathbf{k}_-(\mathbf{k}_- \cdot \mathbf{E}_-) + i\omega_- \omega_p^2 \mathbf{v}_-$$
$$= -(i/2)\omega_- \omega_p^2(n_0 \mathbf{v} + \mathbf{V}_0^* n), \tag{26}$$

$$-i\omega_- \mathbf{v}_- + \mathbf{v}_- \times \boldsymbol{\Omega}_c + \mathbf{E}_- + 3iV_e^2 \mathbf{k}_- n_-$$
$$= -(i/2)\mathbf{k}_- \mathbf{V}_0^* \cdot \mathbf{v} + (i/2)\mathbf{V}_0^* \times (\mathbf{k} \times \mathbf{v} + i\mathbf{B})$$
$$+ \tfrac{1}{2}\mathbf{v} \times (\mathbf{k}_0 \times \mathbf{v}_0 - \mathbf{B}_0), \tag{27}$$

with

$$\mathbf{B} = \mathbf{k} \times \mathbf{E}/\omega, \quad i\mathbf{k} \cdot \mathbf{E} = -\omega_p^2 n.$$

Confining our attention to scattering or decay in the plane perpendicular to the magnetic field $\mathbf{B}_c = B_c\hat{\mathbf{z}}$, then $\mathbf{k}$, $\mathbf{k}_-$, $\mathbf{E}$, $\mathbf{E}_-$, $\mathbf{v}$, $\mathbf{v}_-$ all lie in the (x, y) plane and $\mathbf{B} = B\hat{\mathbf{z}}$. Another independent set is $\{E_z, v_z, B_x, B_y; E_{z-}, v_{z-}, B_{x-}, B_{y-}\}$ which represent decay into two ordinary electromagnetic waves, but phase matching precludes this possibility. Moreover, decay into an upper-hybrid wave and an ordinary wave is not possible. With this choice, Eqs. (24)–(27) have been solved numerically, and the results are discussed in Sec. III.

Recall that the pump wave quantities driving the instabilities are related as follows:

$$E_{0x} = [\Omega_c \omega_p^2/(1 - \omega_p^2 - \Omega_c^2 - 3k_0^2 V_e^2)]E_{0y},$$
$$v_{0x} = -(1/\omega_p^2)E_{0x},$$
$$v_{0y} = [(1 - k_0^2)/\omega_p^2]E_{0y}, \tag{28}$$
$$n_0 = k_0 v_{0x},$$
$$B_0 = k_0 E_{0y},$$

and

$$k_0^2 \simeq [(1-\omega_p^2)^2 - \Omega_c^2]/(1-\omega_p^2-\Omega_c^2). \quad (29)$$

The magnetic field-free dispersion relation, describing the Raman and two-plasmon decay instabilities, emerges in a straightforward manner. When $\Omega_c = 0$, then $E_{0x} = 0 = v_{0x} = n_0 = \mathbf{k}_0 \times \mathbf{v}_0 - \mathbf{B}_0 = \mathbf{k} \times \mathbf{v} + i\mathbf{B} = \mathbf{k}_- \times \mathbf{v}_- + i\mathbf{B}_-$ and $v_{0y} = E_{0y}$, giving

$$\left(\omega^2 - \omega_{es}^2 - \frac{\omega_p^2 k^2}{\omega_-^2 - \omega_{em-}^2} \frac{|\mathbf{k}_- \times \mathbf{v}_0|^2}{4k_-^2}\right) \times \left(\omega_-^2 - \omega_{es}^2 - \frac{\omega_p^2 k_-^2}{\omega^2 - \omega_{em}^2} \frac{|\mathbf{k} \times \mathbf{v}_0|^2}{4k^2}\right) = (\mathbf{k} \cdot \mathbf{v}_0)^2 \frac{(\omega\omega_- k_-^2 + k^2\omega_{es-}^2)(\omega\omega_- k^2 + k_-^2 \omega_{es}^2)}{4\omega\omega_- k^2 k_-^2}$$

$$\simeq (\mathbf{k} \cdot \mathbf{v}_0)^2 [(k^2 - k_-^2)/4kk_-]^2 \quad (\text{when } \omega \simeq \omega_p \simeq \tfrac{1}{2}). \quad (30)$$

Ignoring the right-hand side (or assuming that $\mathbf{k}$ is perpendicular to $\mathbf{v}_0$) yields the Raman dispersion relation. Ignoring the coupling terms on the left-hand side yields the two-plasmon decay dispersion relation. We may safely decouple the two branches since, for a given density, the two instabilities occur in different regions of $(\omega, \mathbf{k})$ space.

From the set of equations (24)–(27) we may obtain the full dispersion relation. It is convenient to first eliminate $\mathbf{B}$ and n, so reducing (24)–(27) to a set of equations for $\{E_x, E_y, v_x, v_y, E_{x-}, E_{y-}, v_{x-}, v_{y-}\}$ from which we may write the dispersion relation

$$|D| = 0, \quad (31)$$

with

$$D = \begin{bmatrix}
(k_y^2 - \omega^2) & -k_x k_y & i\omega\omega_p^2 & 0 & \tfrac{1}{2}\omega k_{x-} v_{0x} & \tfrac{1}{2}\omega k_y v_{0x} & (i/2)\omega\omega_p^2 n_0 & 0 \\
-k_x k_y & (k_x^2 - \omega^2) & 0 & i\omega\omega_p^2 & (i/2)\omega k_{x-} v_{0y} & (i/2)\omega k_y v_{0y} & 0 & (i/2)\omega\omega_p^2 n_0 \\
(1 + 3k_x^2\lambda_D^2) & 3k_x k_y \lambda_D^2 & -i\omega & \Omega_c & -(ik_{x-} v_{0y}/2\omega_-) & (ik_y v_{0y}/2\omega_-) & (i/2)\mathbf{k}\cdot\mathbf{V}_0 & \tfrac{1}{2}k_0 E_{0y} \\
3k_x k_y \lambda_D^2 & (1 + 3k_y^2\lambda_D^2) & -\Omega_c & -i\omega & (k_y v_{0x}/2\omega_-) & (k_{x-} v_{0x}/2\omega_-) & -\tfrac{1}{2}k_0(v_{0y} - E_{0y}) & (i/2)\mathbf{k}_-\cdot\mathbf{V}_0 \\
\tfrac{1}{2}\omega_- k_x v_{0x} & \tfrac{1}{2}\omega_- k_y v_{0x} & (i/2)\omega_-\omega_p^2 n_0 & 0 & (k_{y-}^2 - \omega_-^2) & -k_{x-} k_y & i\omega_-\omega_p^2 & 0 \\
(i/2)\omega_- k_x v_{0y} & (i/2)\omega_- k_y v_{0y} & 0 & (i/2)\omega_-\omega_p^2 n_0 & -k_{x-} k_y & (k_x^2 - \omega_-^2) & 0 & -i\omega_-\omega_p^2 \\
-(ik_x v_{0y}/2\omega) & (ik_y v_{0y}/2\omega) & (i/2)\mathbf{k}_-\cdot\mathbf{V}_0^* & \tfrac{1}{2}k_0 E_{0y} & (1 + 3k_{x-}^2\lambda_D^2) & 3k_{x-} k_y \lambda_D^2 & -i\omega_- & \Omega_c \\
-(k_y v_{0x}/2\omega) & (k_x v_{0x}/2\omega) & \tfrac{1}{2}k_0(v_{0y} - E_{0y}) & (i/2)\mathbf{k}\cdot\mathbf{V}_0^* & 3k_{x-} k_y \lambda_D^2 & (1 + 3k_y^2\lambda_D^2) & -\Omega_c & -i\omega_-
\end{bmatrix}.$$

III. RESULTS

The numerical solutions of the system (24)–(27) are shown in Figs. 1–5. These assume that $(\omega, \mathbf{k})$ is always an electron plasma wave (upper-hybrid when $\Omega_c \neq 0$) while $(\omega_-, \mathbf{k}_-)$ represents either an electron plasma wave (upper-hybrid) in the case of the two-plasmon decay (TPD) or an electromagnetic wave (extraordinary wave) in the case of stimulated Raman scattering (SRS). We shall continue to call the instabilities SRS and TPD even in the presence of the magnetic field since we are considering small fields $\Omega_c \ll 1$, and as such they may be regarded as a perturbation of the unmagnetized problem. The results for each instability are presented differently recognizing their different natures. SRS exists for all densities below $n_c/4$ but is highly localized in k space at any given density. Thus, Figs. 1(a) and (b) show the maximum growth rate (with respect to k_x) and corresponding frequency of the scattered light wave as a function of density (ω_p). By contrast, the TPD is localized near the quarter-critical density region but has a wide spectrum of unstable modes. Figures 2–5 plot the maximum growth rates (w.r.t. ω_p) versus k_x for a variety of k_y values. The results are shown for $\Omega_c = 0$ (solid curve), 0.1 (short-dashed curve), 0.2 (long-dashed curve). Note that $\Omega_c \simeq 0.01 B_{MG}\lambda_{\mu m}$, where B_{MG} is in megagauss and $\lambda_{\mu m}$ is the laser wavelength in microns. In all cases the intensity of the incident radiation is fixed and corresponds to $v_0 = 0.1$ while the electron temperature corresponds to $V_e = 0.1$.

A. Field-free case

Before discussing the effect of the magnetic field on the instabilities, let us fix our ideas by recalling the unmagnetized plasma results which are well understood. Consider

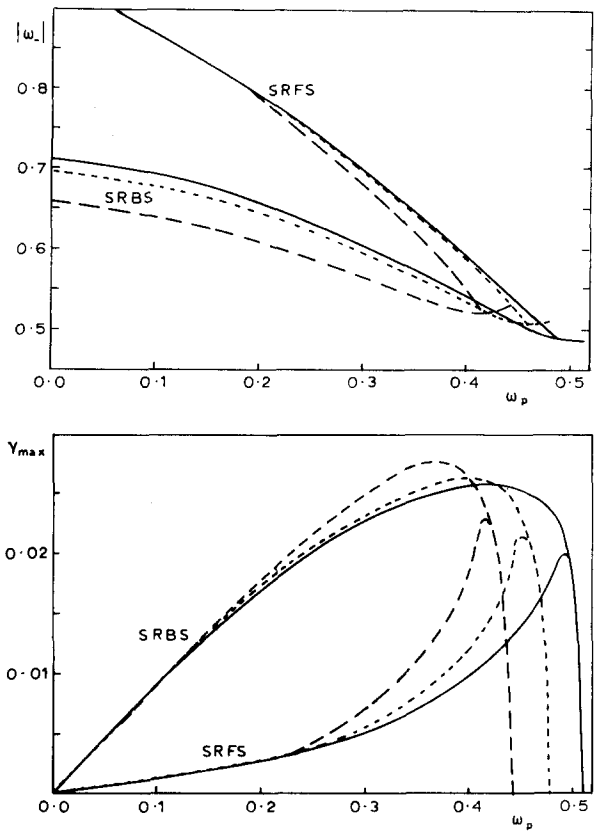

FIG. 1. A plot of (a) the frequencies and (b) the corresponding maximum growth rates for stimulated Raman back (SRBS) and forward (SRFS) scattering ($k_y = 0$). Magnetic fields chosen correspond to $\Omega_c = 0$ (solid line), $\Omega_c = 0.1$ (short-dashed line), and $\Omega_c = 0.2$ (long-dashed line).

first SRS. Its growth rate is[3]

$$\gamma = \omega_p v_0 k k_{x\_} /2k_{\_}, \tag{32}$$

where $k = |\mathbf{k}|$, $k_{\_} = |\mathbf{k}_{\_}|$. Figure 1(a) shows the numerical solution which is accurately given by (32) for exact backscattering and forward scattering ($k_y = 0$). Here, the reflection point of the scattered light wave occurs when $\omega_p^2 = \frac{1}{4} - \frac{3}{8}V_e^2 (\omega_p \simeq 0.489)$ where forward and backscattered waves are indistinguishable. As we move to lower densities, the two branches separate as k varies, for backscatter, from k_0 at $n_c/4$ to $2k_0$ in the very underdense plasma, while for forward scattering k varies from k_0 to ω_p. Of course, for very underdense plasmas ($n \ll n_c/4$), neither result is accurate. For backscattering, $k\lambda_D$ becomes large as ω_p reduces, whence Landau damping becomes severe and SRS degenerates into stimulated Compton scattering. Also, Raman forward scattering becomes a four wave process requiring retention of both Stokes and anti-Stokes components in the dispersion relation. Both effects are omitted here.

For sidescattered emission ($k_y \neq 0$) polarized in the plane perpendicular to $\mathbf{B}_c$, as considered here, the growth rate reduces as $\cos\theta$ where θ is the angle between the electric fields of incident and scattered waves. In fact, when the scattered light wave is at its reflection point it is polarized perpendicular to the incident wave whence the waves are decoupled [$k_y \neq 0$, $k_{x\_} = 0$, and therefore $\gamma = 0$ from (32)]. (Sidescattering, where incident and scattered light waves are polarized parallel to one another, will be published later.) As k_y increases, so the maximum resonant density decreases. This necessarily requires k_y to be less than unity.

Next, consider the two-plasmon decay instability. This is inherently two-dimensional and, of course, does not appear in unmagnetized plasmas when $k_y = 0$. Its growth rate is[10]

$$\gamma = \omega_p v_0 k_0 k_y K /2k\, k_{\_}, \quad k_x = k_0/2 + K. \tag{33}$$

This maximizes when $K^2 = k_y^2 + k_0^2/4$, so that

$$\gamma = \omega_p k_0 v_0/2. \tag{34}$$

The resonant density is

$$\omega_p^2 = \tfrac{1}{4} - (3V_e^2/2)(k^2 + k_{\_}^2). \tag{35}$$

Equations (33)–(35) agree with the numerical solutions (cf. Figs. 3–5) of the fully electromagnetic result, Eq. (31). Note also the expected symmetry about $k_0/2 (\simeq 0.43)$ of the TPD which appears in Figs. 3–5.

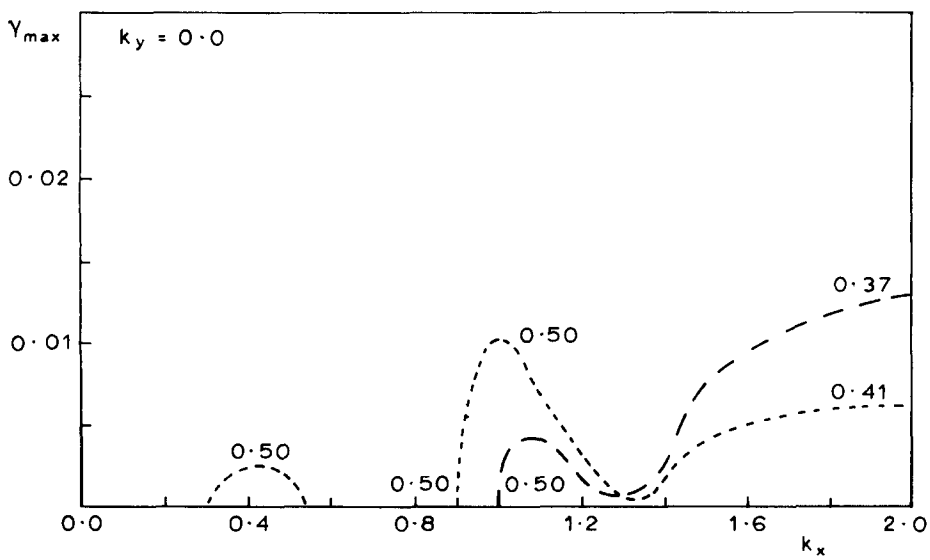

FIG. 2. Maximum growth rates (with respect to density) for two-plasmon decay as functions of k_x at a given k_y. Magnetic fields chosen correspond to $\Omega_c = 0.1$ (short-dashed line), $\Omega_c = 0.2$ (long-dashed line); $v_0 = 0.1$, $V_e = 0.1$, $k_y = 0.0$.

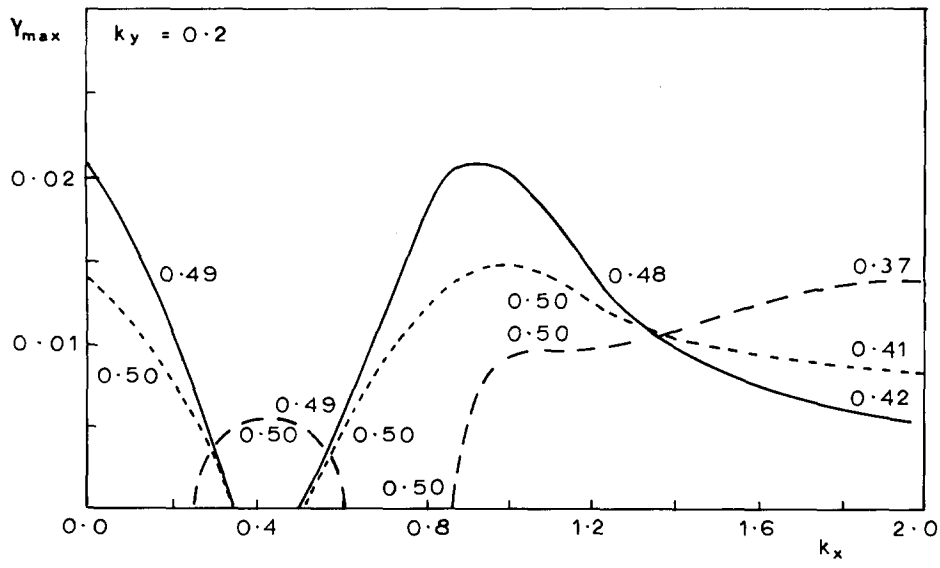

FIG. 3. Maximum growth rates (with respect to density) for two-plasmon decay as functions of k_x at a given k_y. Magnetic fields chosen correspond to $\Omega_c = 0.0$ (solid line), $\Omega_c = 0.1$ (short-dashed line), and $\Omega_c = 0.2$ (long-dashed line); $v_0 = 0.1$, $V_e = 0.1$, $k_y = 0.2$.

B. Magnetized case

The magnetic field alters the physics in two ways, both of which are due to the fact that no waves are purely electrostatic or electromagnetic. First, the two-plasmon decay may occur in one dimension ($k_y = 0$). Second, at the reflection point (where absolute instability is expected in an inhomogeneous plasma) of the sidescattered ($k_y \neq 0$) extraordinary wave, the magnetic field now makes the growth qualitatively and quantitatively similar to the backscattering results. This is because the incident and scattered extraordinary waves are no longer polarized perpendicular to one another. Thus, the magnetic field tends to destroy the characteristic polarization of SRS emission.

In addition, the magnetic field induces changes in both the real part of the frequency and in the growth rate. First, consider the frequency shifts which are easily deduced from phase matching arguments. The dispersion relation describing the extraordinary and upper-hybrid waves, (11), gives

$$\omega^2 = \tfrac{1}{2}(\omega_{es}^2 + \omega_{em}^2) \pm [\tfrac{1}{4}(\omega_{es}^2 - \omega_{em}^2)^2 + \Omega_c^2 \omega_p^2]^{1/2}, \tag{36}$$

where

$$\omega_{es}^2 = \omega_p^2 + \Omega_c^2 + 3k^2 V_e^2, \tag{37}$$

$$\omega_{em}^2 = \omega_p^2 + k^2. \tag{38}$$

Assuming $\Omega_c \ll \omega_p$ and $k^2 \gg 2\Omega_c \omega_p$, then

$$\omega^2 \simeq \omega_p^2 + 3k^2 V_e^2 + \Omega_c^2 (1 - \omega_p^2/k^2) \quad \text{(upper hybrid)}, \tag{39}$$

or

$$\omega^2 \simeq \omega_p^2 + k^2 + \Omega_c^2 \omega_p^2 / k^2 \quad \text{(extraordinary)}. \tag{40}$$

For the two-plasmon decay with $1 = \omega_1 + \omega_2$, $\mathbf{k}_0 = \mathbf{k}_1 + \mathbf{k}_2$, both decay waves are described by (39), i.e.,

$$\omega_1 = \frac{1}{2} + k_0 K \left(3V_e^2 + \frac{\omega_p^2 \Omega_c^2}{k_1^2 k_2^2} \right) \quad \left(k_{x1} = \frac{k_0}{2} + K \right). \tag{41}$$

The magnetic field, therefore, serves to increase the shift of both decay products from $\frac{1}{2}$, symmetry still being preserved. These shifts are electromagnetic in origin. The magnetic

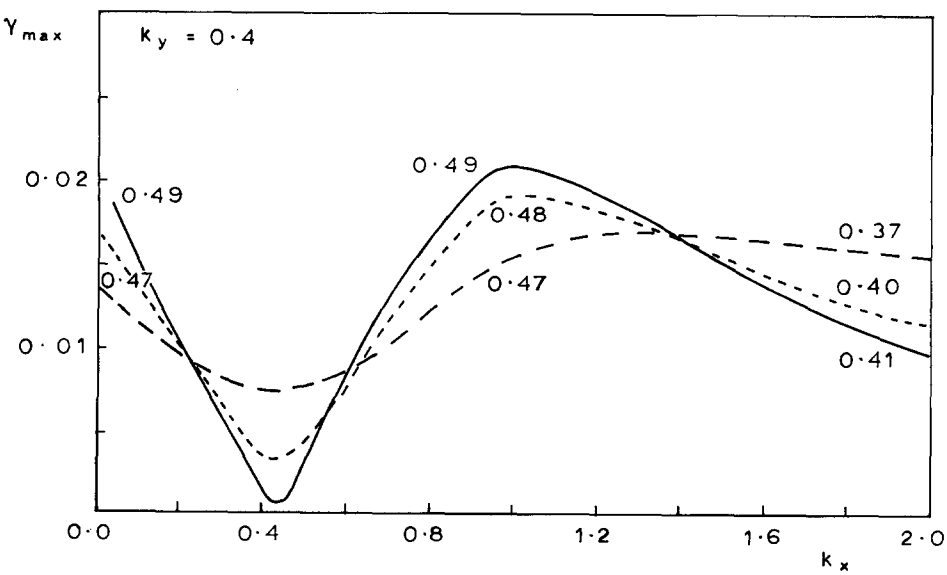

FIG. 4. Maximum growth rates (with respect to density) for two-plasmon decay as functions of k_x at a given k_y. Magnetic fields chosen correspond to $\Omega_c = 0.0$ (solid line), $\Omega_c = 0.1$ (short-dashed line), and $\Omega_c = 0.2$ (long-dashed line); $v_0 = 0.1$, $V_e = 0.1$, $k_y = 0.4$.

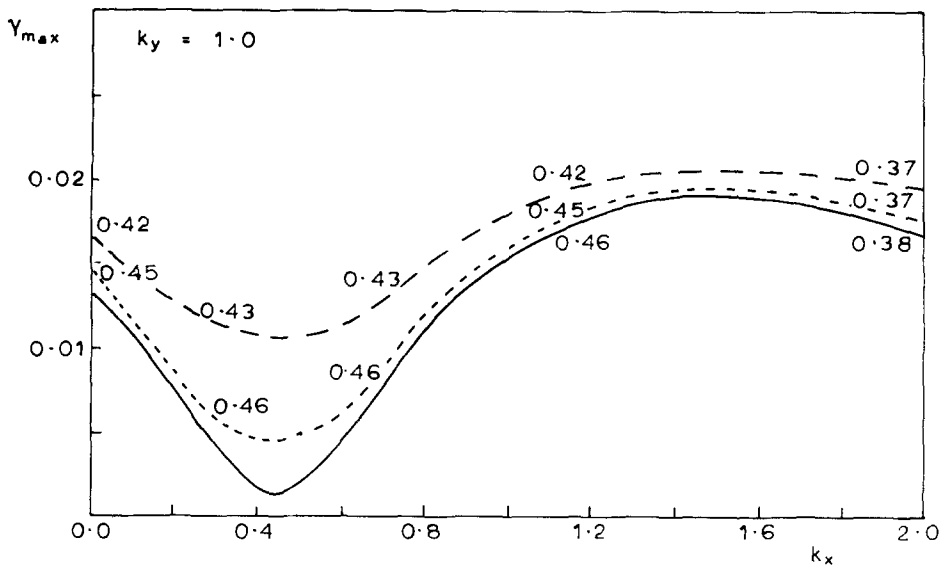

FIG. 5. Maximum growth rates (with respect to density) for two-plasmon decay as functions of k_x at a given k_y. Magnetic fields chosen correspond to $\Omega_c = 0.0$ (solid line), $\Omega_c = 0.1$ (short-dashed line), and $\Omega_c = 0.2$ (long-dashed line); $v_0 = 0.1$, $V_e = 0.1$, $k_y = 1.0$.

field induced shift $\delta\omega_B$ can be of the same order as, or greater than, the thermal shift $\delta\omega$ for sufficiently large fields. For example, in Fig. 4 ($k_y = 0.4$, $\omega_p = 0.48$) maximum growth occurs when $k_x \simeq 1$, so that $\delta\omega_B \simeq 0.56\Omega_c^2$ while $\delta\omega \simeq 0.015$. The numerical results agree with these expressions. The position of the resonance is given by

$$\omega_p^2 = \frac{1}{4} - \left(k_y^2 + K^2 + \frac{k_0^2}{4}\right)\left(3V_e^2 - \frac{\Omega_c^2\omega_p^2}{k_1^2 k_2^2}\right) - \Omega_c^2. \tag{42}$$

If we assume that maximum growth is still given approximately when $K^2 = k_y^2 + k_0^2/4$, then the resonant density is increased by the magnetic field by an amount given by

$$(1/8k_y^2 - 1)\Omega_c^2. \tag{43}$$

These are small changes unless k_y is very small; however, this behavior is observed in the numerical solutions. As we shall see, the maximum growth occurs at larger K.

For stimulated Raman scattering, consider the frequency shift induced by the magnetic field for backscatter ($k_y = 0$) at the reflection point ($k_{2x} = 0$) of the extraordinary wave. From (36), with $k_2 = 0$,

$$\omega_2^2 = \omega_p^2 + \Omega_c^2/2 + (\Omega_c^4/4 + \Omega_c^2\omega_p^2)^{1/2}. \tag{44}$$

Thus, when $\Omega_c \ll \omega_p$,

$$\omega_2 \simeq \omega_p + \Omega_c/2, \tag{45}$$

and

$$\omega_1 \simeq 1 - \omega_p - \Omega_c/2 \quad \text{or} \quad \omega_p \simeq 1 - \omega_1 - \Omega_c/2, \tag{46}$$

which, in (39) yields

$$\omega_1^2 = (1 - \omega_1 - \Omega_c/2)^2 + 3k_0^2 V_e^2 + \Omega_c^2(1 - \omega_p^2/k_0^2). \tag{47}$$

Then

$$\omega_1 \simeq \frac{1}{2} + \frac{9V_e^2}{8} - \frac{\Omega_c}{4}, \tag{48}$$

to first order in Ω_c and using $k_0^2 \simeq \frac{3}{4}$; also,

$$\omega_p \simeq \frac{1}{2} - \frac{9V_e^2}{8} - \frac{\Omega_c}{4}. \tag{49}$$

Thus we have a linear downshift $\delta\omega_B$ of the frequency of the upper-hybrid wave (a shift to the blue in the scattered extraordinary wave) because of the magnetic field, which can easily reverse the thermal shift $\delta\omega$. For example, with $V_e = 0.1$, $\Omega_c = 0.1$, then $\delta\omega \simeq 0.01$ while $\delta\omega_B \simeq -0.025$. Thus an expected red shift of the scattered light of the Raman instability can readily turn into a blue shift in the presence of a large enough self-generated magnetic field. Figure 1(a) shows this behavior near $n_c/4$. This frequency shift arises solely from the electrostatic component in the scattered extraordinary wave. This shift is particularly relevant when one considers that it occurs at the reflection point, where absolute instability is expected. Moving to lower densities, the decay waves become more purely electrostatic or electromagnetic in nature. So, for backscatter, the frequency shift shown in Fig. 1(a) is entirely caused by the magnetic field contribution to the upper-hybrid frequency.

Figure 1(b) shows that the magnetic field increases the growth rate of both Raman forward and backscattering while moving the location of the resonance to lower densities. For sidescattering growth reduces with increasing k_y as in the unmagnetized case except that at the scattered wave reflection point the growth rate increases from zero when $\Omega_c = 0$ to be qualitatively like Fig. 1(b) when $\Omega_c = 0.1, 0.2$. For a given k_y, the magnetic field increases growth rates.

The two-plasmon decay growth rates are unequivocally increased by the magnetic field when k_y is large enough. Figure 5 shows the increase for $k_y = 1$ for all of a wide range of wavenumbers. Maximum growth still occurs where $K^2 = k_y^2 + k_0^2/4$ ($k_x = k_0/2 + K$) as in the unmagnetized case. For smaller values of k_y the behavior is more complex as shown in Figs. 2–4. For instance, these figures show the possibility of decay into two forward propagating upper-hybrid waves with $k_x \simeq k_0/2$. ($\simeq 0.43$).

IV. CONCLUSIONS

The effects of a magnetic field on the Raman and two-plasmon decay instabilities have been examined in the neighborhood of the quarter-critical density, where the instabili-

ties are coincident, by solving the full set of Maxwell's equations. We have shown that the Raman growth rates are increased in a magnetized plasma. The behavior of the two-plasmon growth rates is more complex in that they are lower in a magnetized plasma than in the field-free case for small values of k_y ($k_y \leq 0.7$) near wavenumbers k_x corresponding to the maximum field-free growth rate, but are enhanced at all wavelengths for $k_y \geq 0.7$. These results are in contrast to those of Grebogi and Liu[31,32] who treated the upper-hybrid wave electrostatically and concluded that both Raman and two-plasmon decay growth rates decreased with magnetic field. Although we believe their model equations to be correct, they omitted terms of order Ω_c in their attempt to derive a simple analytic expression. Our model indicates a complex k dependence which reverses their conclusions.

From the real part of the dispersion relations we have determined frequency shifts in the two processes because of the magnetic field. For the two-plasmon decay the frequency shift from $\omega_0/2$ is increased by the magnetic field by amounts which can exceed the thermal shift. This shift is a consequence of the electromagnetic correction to the dispersion relation and so does not appear in the electrostatic approximation used by Grebogi and Liu.[32] For the Raman instability, the frequency shift of the backscattered wave caused by the magnetic field can change the expected thermal red shift into a blue shift. These results are of particular interest in connection with the generation of radiation at the half-harmonic frequencies referred to in the introduction, and these will be discussed in a future publication. The principal consequence for the emission at $3\omega_0/2$ is that the separation of the red and blue wings now depends on both electron temperature and magnetic field intensities. If one could determine the temperature independently, then this separation could be used to estimate magnetic field strengths near quarter-critical.

There are a number of limitations to the analysis presented in this paper insofar as it relates to laser–plasma interactions. We have taken the plasma to be homogeneous and have supposed that the magnetic field $\mathbf{B}_c$ is both constant and uniform, even though we know that in reality self-generated magnetic fields have a rather complex morphology.[24,33] However, we believe it to be a justifiable first step, particularly since *detailed* density and magnetic field profiles are not known experimentally. Moreover, in the theoretical treatment itself we have used a fluid model to describe the plasma, which would be better described by a kinetic theoretic treatment. This is in hand.

[1]D. W. Forslund, J. M. Kindel, and E. L. Lindman, Phys. Rev. Lett. **30**, 739 (1973).
[2]J. F. Drake, P. K. Kaw, Y. C. Lee, G. Schmidt, C. S. Liu, and M. N. Rosenbluth, Phys. Fluids **17**, 778 (1974).
[3]C. S. Liu, M. N. Rosenbluth, and R. B. White, Phys. Fluids **17**, 1211 (1974).
[4]D. Biskamp and H. Welter, Phys. Rev. Lett. **34**, 312 (1975).
[5]W. L. Kruer, K. Estabrook, B. F. Lasinski, and A. B. Langdon, Phys. Fluids **23**, 1326 (1980).
[6]M. V. Goldman, Ann. Phys. (N.Y.) **38**, 117 (1966).
[7]E. A. Jackson, Phys. Rev. **153**, 235 (1967).
[8]M. N. Rosenbluth, Phys. Rev. Lett. **29**, 565 (1972).
[9]Y. C. Lee and P. K. Kaw, Phys. Rev. Lett. **32**, 135 (1974).
[10]C. S. Liu and M. N. Rosenbluth, Phys. Fluids **19**, 967 (1976).
[11]J. J. Schuss, Phys. Fluids **20**, 1120 (1977).
[12]A. B. Langdon, B. F. Lasinski, and W. L. Kruer, Phys. Rev. Lett. **43**, 133 (1979).
[13]H. A. Baldis, J. C. Samson, and P. B. Corkum, Phys. Rev. Lett. **41**, 1719 (1978).
[14]S. Jackel, J. Albritton, and E. Goldman, Phys. Rev. Lett. **35**, 514 (1975).
[15]H. C. Pant, K. Eidmann, P. Sachensmaier, and R. Sigel, Opt. Commun. **16**, 396 (1976).
[16]V. V. Aleksandrov, S. I. Anisimov, M. V. Brenner, E. P. Velikhov, V. P. Vikharev, V. P. Zotov, N. G. Kovalskii, M. I. Pergament, and A. I. Yaroslavskii, Zh. Eksp. Teor. Fiz. **71**, 1826 (1976) [Sov. Phys. JETP **44**, 958 (1977)].
[17]V. Y. Bychenkov, V. P. Silin, and V. T. Tikhonchuk, Fiz. Plazmy **3**, 1314 (1977) [Sov. J. Plasma Phys. **3**, 730 (1977)].
[18]P. D. Carter, S. M. L. Sim, H. C. Barr, and R. G. Evans, Phys. Rev. Lett. **44**, 1407 (1980).
[19]A. I. Avrov, V. Yu. Bychenkov, O. N. Krokhin, V. V. Pustovalov, A. A. Rupasov, V. P. Silin, G. V. Sklizkov, V. T. Tikhonchuk, and A. S. Shikanov, Zh. Eksp. Teor. Fiz. **72**, 970 (1977) [Sov. Phys. JETP **45**, 507 (1977)].
[20]J. A. Stamper, K. Papadopoulos, S. O. Dean, E. A. McLean, and J. M. Dawson, Phys. Rev. Lett. **26**, 1012 (1972).
[21]J. A. Stamper and B. H. Ripin, Phys. Rev. Lett. **34**, 138 (1975).
[22]J. A. Stamper, E. A. McLeans, and B. H. Ripin, Phys. Rev. Lett. **40**, 1177 (1978).
[23]A. Raven, O. Willi, and P. T. Rumsby, Phys. Rev. Lett. **41**, 554 (1978).
[24]A. Raven, P. T. Rumsby, J. A. Stamper, O. Willi, R. Illingworth, and R. Thareja, Appl. Phys. Lett. **35**, 526 (1979).
[25]O. Willi, A. Raven, and P. T. Rumsby, Phys. Lett. A **71**, 435 (1979).
[26]J. Weiland and H. Wilhelmsson, *Coherent Nonlinear Interaction of Waves in Plasmas* (Pergamon, Oxford, 1977).
[27]M. Porkolab, Physica B, C **82**, 86 (1976).
[28]T. J. M. Boyd and J. G. Turner, J. Math. Phys. **19**, 1403 (1978).
[29]L. Stenflo, Plasma Phys. **16**, 677 (1974).
[30]P. K. Kaw, Adv. Plasma Phys. **6**, 207 (1976).
[31]C. Grebogi and C. S. Liu, Phys. Fluids **23**, 1330 (1980).
[32]C. Grebogi and C. S. Liu, J. Plasma Phys. **23**, 147 (1980).
[33]T. J. M. Boyd, G. J. Humphreys-Jones, and D. Cooke, Phys. Lett. A **88**, 140 (1982).